Thermal transport in disordered one-dimensional spin chains

Igor Poboiko and Mikhail Feigel'man
L. D. Landau Institute for Theoretical Physics, 117940 Moscow, Russia
and Moscow Institute for Physics and Technology, Dolgoprudny, Moscow region, Russia
(Received 3 September 2015; revised manuscript received 28 October 2015; published 31 December 2015)

We study a one-dimensional anisotropic XXZ Heisenberg spin-$\frac{1}{2}$ chain with weak random fields $h_i^z S_i^z$ by means of Jordan-Wigner transformation to spinless Luttinger liquid with disorder and bosonization technique. First, we reinvestigate the phase diagram of the system in terms of dimensionless disorder $\gamma = \langle h^2\rangle/J^2 \ll 1$ and anisotropy parameter $\Delta = J_z/J_{xy}$, we find the range of these parameters where disorder is irrelevant in the infrared limit and spin-spin correlations are described by power laws, and compare it with previously obtained numerical and analytical results. Then we use the diagram technique in terms of plasmon excitations to study the low-temperature ($T \ll J$) behavior of heat conductivity κ and spin conductivity σ in this power-law phase. The obtained Lorentz number $L \equiv \kappa/\sigma T$ differs from the value derived earlier by means of the memory function method. We argue also that in the studied region inelastic scattering is strong enough to suppress quantum interference in the low-temperature limit.

DOI: 10.1103/PhysRevB.92.235448 PACS number(s): 73.90.+f, 75.10.Pq

I. INTRODUCTION

The one-dimensional disordered spin chain is an excellent example of a strongly correlated quantum system that is well suited to study the basic properties of such systems. In particular, the studies of disordered spin chains have become one of the major playgrounds in the field of many-body localization (MBL) [1–8]. From the experimental viewpoint, quasi-one-dimensional antiferromagnets [9–11] attract considerable attention due to their very high thermal conductance, which is believed to be related with the integrability of the clean Heisenberg spin-$\frac{1}{2}$ chain [12,13]. It is known since the seminal paper of Ref. [14] that in 1D the competition between interaction and disorder may lead to delocalization and the formation of a ground state that is nearly-free from the effects of disorder, see also Refs. [15,16]. Numerical studies [17–19] confirm that qualitative conclusion. In order to provide delocalization, the interaction should be sufficiently strong and attractive, so this problem bears some resemblance with a model of superconductor-insulator transition in higher-dimensional systems [20]. Looking from that perspective, it seems useful to develop a quantitative theory of the delocalized phase of one-dimensional quantum systems with a bare disorder that is "screened" by interactions. In particular, it is important to study heat transport in a system that is expected to be dominated by the remains of the disorder potential.

Here we will study the properties of anisotropic XXZ spin chains in a random magnetic field along the z direction, which is described by the Hamiltonian (we assume $J > 0$)

$$\hat{H} = -J \sum_n \left(\hat{S}_n^x \hat{S}_{n+1}^x + \hat{S}_n^y \hat{S}_{n+1}^y + \Delta \hat{S}_n^z \hat{S}_{n+1}^z + \frac{h_n}{J} \hat{S}_n^z \right). \quad (1)$$

By means of the Jordan-Wigner (JW) transformation the Hamiltonian (1) can be reduced to the Hamiltonian of interacting spinless fermions (here $\rho_n = c_n^\dagger c_n - \frac{1}{2}$):

$$\hat{H} = -J \sum_n \left(\frac{1}{2} c_n^\dagger c_{n+1} + \text{H.c.} + \Delta \rho_n \rho_{n+1} + \frac{h_n}{J} \rho_n \right). \quad (2)$$

The anisotropy parameter Δ can be both positive and negative, which corresponds to the effective attraction or repulsion between JW fermions, respectively.

We will consider random fields that are relatively small, so that $\gamma = \langle h^2\rangle/J^2 \ll 1$, and have zero average $\langle h\rangle = 0$. Thus our system is, on average, symmetric with respect to $z \mapsto -z$ reflection, which translates into the particle-hole symmetry in terms of JW fermions. It ensures that in the quasiparticle spectrum $\varepsilon(k)$ only odd powers of k survive.

The goal of this paper is to study low-temperature (i.e., the range $T \ll J$) transport properties, spin and heat conductivity, in the range of parameters (Δ, γ) where $T = 0$ spin-spin correlations decay as a power law with the distance. The rest of the paper is organized as follows. In Sec. II, we study the phase diagram by means of renormalization group (RG) approach formulated in Ref. [14]. Although a similar study was performed in Ref. [17], we need to expose the RG approach here for completeness of the discussion and for a comparison with the currently available numerical data. Section III is devoted to the formulation and an application of the Keldysh approach to the transport properties of disordered Luttinger liquid model, which is an appropriate low-energy approximation for the lattice fermion model (2); in Sec. III A, spin and heat conductivities (σ and κ) are studied within the region $\frac{1}{2} \leqslant \Delta \leqslant 1$ where disorder is irrelevant in the RG sense; next, in Sec. III B, we discuss the specific behavior of σ and κ near the critical point $\Delta = \frac{1}{2}$; the role of quantum interference corrections and decoherence is discussed in Sec. III C, and the role of spectrum nonlinearity is considered in Sec. III D. Finally, we present our conclusions in Sec. IV.

II. LUTTINGER LIQUID DESCRIPTION AND PHASE DIAGRAM

In the clean limit $h_n = 0$ and in the region $-1 < \Delta < 1$, the excitation spectrum of the interacting one-dimensional fermion system (2) is gapless; then the low-energy and long-distance properties of the system are known to be described by the Luttinger liquid (LL) model [15]. It allows to rewrite the Hamiltonian in terms of fermion density excitations—

plasmons. The LL model is formulated in terms of canonically conjugated plasmon fields $[\phi(x),\Pi(y)] = i\delta(x-y)$; in the linear approximation for the quasiparticle spectrum, the Hamiltonian of the LL model reads

$$\hat{H}_{LL} = \frac{1}{2\pi}\int dx\left(\frac{u}{K}(\partial_x\phi)^2 + uK(\pi\Pi)^2\right). \tag{3}$$

Here, u is the plasmon velocity and K is a dimensionless Luttinger parameter; these parameters are determined, via the Bethe ansatz solution for the XXZ model, by the values of J and Δ, see Ref. [15], p. 167:

$$\Delta = \cos\frac{\pi}{2K}, \quad u = \frac{Ja}{2}\frac{\sin(\pi/2K)}{1-1/2K}, \tag{4}$$

where a is the lattice constant.

In our model (2) disorder couples to the fermion density ρ_n; in the LL continuum limit, it reads as $\rho(x) = -\frac{1}{\pi}\partial_x\phi + \frac{1}{\pi a}\cos(2k_F x - 2\phi)$. The first and second terms in the above expression correspond to the slow ($q \sim 0$) and fast oscillating ($q \sim 2k_F$) parts. Thus there are two types of scattering of one-dimensional fermions by disorder: forward and backward. Forward scattering is irrelevant within the linear approximation for the spectrum, since the corresponding term in the LL Hamiltonian can be eliminated completely by the redefinition of phase $\phi(x)$. The backward fermion scattering with momentum transfer $q \sim 2k_F$ is the only effect one should take into account then. Thus we need only the $q \sim 2k_F$ part of the original random potential; this part is described by the random Gaussian complex field $\xi(x)$ with $\langle\xi(x)\xi^*(y)\rangle = D\delta(x-y)$ and $D = \langle h^2\rangle a$. The disorder contribution to the Hamiltonian reads as follows:

$$\hat{H}_{\rm dis} = -\frac{1}{2\pi\alpha}\int dx(\xi(x)e^{-2i\phi} + \xi^*(x)e^{2i\phi}). \tag{5}$$

The renormalization group approach to a disordered Luttinger liquid was formulated in Ref. [14]. It is convenient to introduce a dimensionless disorder parameter:

$$g = \frac{2Da}{\pi u^2} = \frac{8(1-1/2K)^2}{\pi\sin^2(\pi/2K)}\gamma. \tag{6}$$

In terms of this parameter and logarithmic scaling parameter $\xi = \ln\frac{\tilde{a}}{a}$ (with $\tilde{a}$ being running ultraviolet cutoff), the RG equations read as follows:

$$\begin{aligned}\frac{du}{d\xi} &= -\frac{uK}{2}g\\ \frac{dK}{d\xi} &= -\frac{K^2}{2}g\\ \frac{dg}{d\xi} &= (3-2K)g.\end{aligned} \tag{7}$$

These equations can be solved analytically exploiting their first integral $I(K,g) = \frac{9}{8}(\frac{6}{K} + 4\ln K - g)$. The prefactor 9/8 in the definition of $I(K,g)$ helps to present the parameter α (measuring distance to the transition line, see Sec. III B) in a more convenient form. This solution yields the phase diagram shown as a solid line in Fig. 1. The "delocalized" region lies, in the limit of very weak disorder, in the range $\frac{1}{2} < \Delta < 1$. Upon increase of γ, the delocalized region shrinks and eventually disappears already at $\gamma \approx 0.1$. Everywhere in the delocalized phase the effective disorder $g(\xi)$ decreases with ξ.

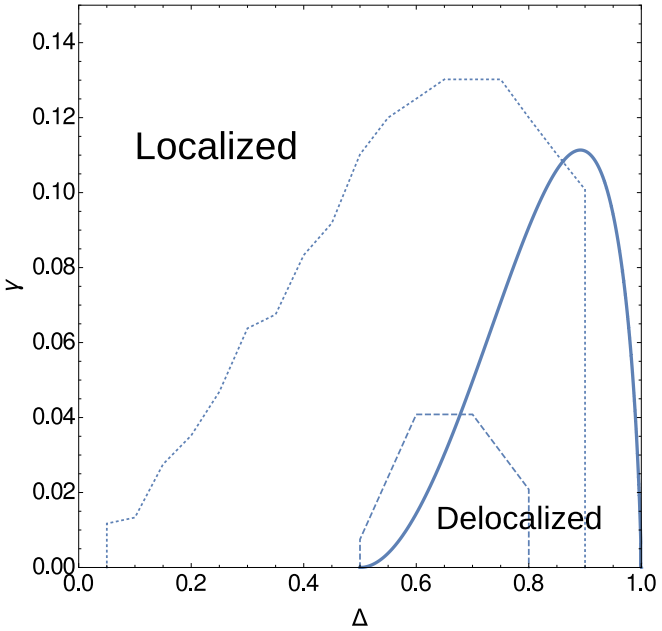

FIG. 1. (Color online) Approximate phase diagram for a disordered XXZ spin chain. Solid line: the one found from the RG calculations for the Luttinger liquid model with a linear spectrum (originally obtained in Ref. [17] with wrong scale along γ). The small area under the dashed line corresponds to the phase boundary presented in Ref. [18]; the large area under the dotted line corresponds to the phase boundary presented in Ref. [19].

Equal-time spin-spin correlation function $\langle S^+(0)S^-(x)\rangle$ decays as a power law at $\Delta > \frac{1}{2}$, as one can read in Ref. [16], where a two-loop RG calculation was performed. At smaller $\Delta < \frac{1}{2}$, the renormalized disorder parameter $g(\xi)$ grows with ξ, and one expects an exponential decay of $\langle S^+(0)S^-(x)\rangle$ at $x \geqslant L_c$, where the correlation length

$$L_c = c(K)\gamma^{1/(2K-3)}; \quad c(1) \approx 2, \tag{8}$$

see Ref. [14]. Note that for the case of the XY model with random fields along the z axis (i.e. $\Delta = 0$) an exponential decay of $\langle S^+(0)S^-(x)\rangle$ follows directly from single-particle localization in 1D, as proven rigorously in Ref. [21]. However, for any $\Delta < \frac{1}{2}$, the relation between the growth of effective disorder upon RG and Anderson localization is far from being obvious, since the RG calculation [14] does not contain any multiple-impurity interference effects, see Refs. [22,23]. The value of $c(K=1) \approx 2$ follows from a well-known result [24] for the localization length in the one-dimensional Anderson problem, $L_{\rm loc} = 96/W^2$, see Eq. (9) below for the relation between W and γ; we expect $c(K)$ to be a slow function of K on the interval $K \in (1,2)$.

Actually, the derivation of the RG equations (7) as it was performed in Ref. [14] is valid quantitatively in the vicinity of the point $K = 3/2$ only, where the disorder-induced corrections to the parameter K are logarithmic; for a large K, these equations can be used for a qualitative analysis only (the above-mentioned limitation is specific for the effects of distributed disorder and is not relevant for LL with a single

impurity, like the one studied in Ref. [26]). Note that the drop of the critical disorder γ near the point $\Delta = 1$ is trivially related to the decrease of the effective Luttinger velocity u, see Eqs. (4) and (6). However, at large K, i.e., small $1 - \Delta$, some effects related to the nonlinearity of the excitation spectrum (neglected within the standard LL model) become increasingly important. We present some arguments related to those effects towards the end of the paper. Here, we just note that low-lying single-particle excitations at the isotropic point $\Delta = 1$ are *exactly* described by magnons with the spectrum $\epsilon(q) = Ja^2q^2$, with $qa \ll 1$, and a random potential h_n leads to their straightforward localization.

A similar phase diagram was originally obtained in Ref. [17]. However, the definition of group velocity u in Ref. [17] differs from the one given by (4) by a factor of two, resulting in a four-times extension of the phase diagram along the γ axis, as was noticed already in Ref. [18]. A simple check of Eq. (4) can be performed at point $\Delta = 0$, $K = 1$, where the fermion spectrum is known exactly to be $\epsilon(k) = -J\cos(ka)$, yielding a Fermi velocity $v_F = Ja$, which coincides with (4), while Ref. [17] yields $v_F = 2Ja$.

The phase diagram obtained by the analysis of RG equations can be compared with the numeric phase diagram from Ref. [18], see dashed line in Fig. 1. Comparing Eq. (2) with the Eq. (1) of Ref. [18], one obtains the following correspondence between parameters:

$$J = 2, \quad \gamma = \frac{W^2}{48}, \quad \Delta = -V/2. \tag{9}$$

Using these equations, we obtain a phase boundary that is shown by the dashed line in Fig. 1. According to these numerical data, the delocalized region covers a much smaller part of the phase diagram than the RG calculations predict. We expect that the major source of this discrepancy is due to inapplicability of the RG equations (7) at large K values due to the effects of spectrum nonlinearity that becomes important closer to $\Delta = 1$. On the other hand, near the point $K = 3/2$, the numerical data [18] suggest delocalization at the values of γ that are above our critical line. We believe that this discrepancy comes from the limited accuracy of the numerical data due to finite size effects, which becomes most prominent at very weak disorder; the same effect in a more prominent form is discussed below in connection with the results of Ref. [19].

A disorder-interaction phase diagram for the 1D fermion model was also obtained in Ref. [19], see the dotted line in Fig. 1 [the notations here are almost the same as in Ref. [18], up to the change $V \to U$, so we can use (9)]. The delocalized region obtained in Ref. [19] is noticeably larger than the one predicted by RG equations (7). The delocalized phase appears when $\gamma \lesssim 0.13$, which is close to the predicted $\gamma \lesssim 0.10$; however, the delocalized region is much wider and spreads almost up to the noninteracting point $\Delta = 0$, which strongly disagrees with the predicted value of $\Delta = 0.5$. We argue that such behavior of transition line can be caused by finite-size effects. To support this argument, we should estimate the localization length using Eq. (8) and compare it with the maximal system size used in the computations of Ref. [19]. For example, consider the point $\Delta = 0.3$ and $W = 1.4$ (that corresponds to $K \approx 1.24$ and $\gamma \approx 0.045$, close to the phase boundary of Ref. [19]); our estimate (8) yields $L_{\rm loc} \approx 400$, which is comparable to the maximal system sizes $L \approx 1000$ used. In other terms, the large value of the exponent $(3-2K)^{-1}$ for K slightly less than $3/2$, and the smallness of the relevant dimensionless disorder parameter γ, lead to a very small inverse correlation length $1/L_{\rm loc}$ that is difficult to distinguish from zero within numerical analysis. Below, we will focus on the delocalized phase $\frac{1}{2} < \Delta < 1$ that corresponds to the range of $\frac{3}{2} < K < \infty$, where the renormalized disorder constant g is small, and one can obtain transport properties using perturbation theory for the bosonic LL model with renormalized parameters.

III. TRANSPORT PROPERTIES

Here, we proceed from the Hamiltonian description defined by Eq. (3.5) to the Keldysh action for the LL model with disorder. We follow Ref. [25], introducing a Keldysh time contour with time running from minus infinity to plus infinity and backwards. The total Keldysh action $S_{\rm tot}$ consists of a trivial free boson part S_0 and a disorder-related part coming directly from Eq. (5):

$$S_{\rm dis} = \frac{1}{2\pi a}\int_C dtdx(\xi(x)e^{-2i\phi} + \xi^*(x)e^{2i\phi}). \tag{10}$$

We integrate $\exp(iS_{\rm tot})$ over a random Gaussian field $\xi(x)$ and perform a Keldysh rotation introducing classical $\phi_{cl} = \frac{1}{2}(\phi_+ + \phi_-)$ and quantum $\phi_q = \phi_+ - \phi_-$ field components, arriving finally at the effective disorder action

$$S_{\rm dis} = \frac{iD}{\pi^2a^2}\int dt_1dt_2dy\cos 2(\phi_{cl}(y,t_1) - \phi_{cl}(y,t_2)) \times \sin\phi_q(y,t_1)\sin\phi_q(y,t_2). \tag{11}$$

The integration dy over the single coordinate y comes about due to the averaging over the δ-correlated random potential $\xi(x)$.

The corresponding vertex coming from Keldysh action (11) is highly nonlinear. In order to apply Wicks theorem with such a vertex, one needs to Taylor-expand the corresponding nonlinear term and perform a contraction and then a resummation of the series. However, one can note that such a procedure is effectively equivalent to taking a derivative with respect to the corresponding ϕ field, e.g., $\langle\phi(\mathbf{x}_1)f(\phi(\mathbf{x}_2))\rangle = \langle\phi(\mathbf{x}_1)\phi(\mathbf{x}_2)\rangle \times \langle\frac{\partial f}{\partial\phi}(\phi(\mathbf{x}_2))\rangle$.

In order to obtain the self-energy for the retarded Green function in the lowest order over $S_{\rm dis}$ we consider the first-order correction to it, which reads

$$\begin{aligned} i\delta G_R^{(1)}(t-t',x-x') &= \frac{iD}{\pi^2\alpha^2}\int dt_1dt_2dy\langle\phi_{cl}(x,t)\phi_q(x',t') \\ &\times\cos 2(\phi_{1cl}-\phi_{2cl})\sin\phi_{1q}\sin\phi_{2q}\rangle_0 \\ &= \frac{4iD}{\pi^2\alpha^2}\int dt_1dt_2dyG_R^{(0)}(x-y,t-t_1) \\ &\times\left(G_R^{(0)}(t_1-t',y-x') - G_R^{(0)}(t_2-t',y-x')\right) \\ &\times\langle\sin 2(\phi_{cl}(y,t_1)-\phi_{cl}(y,t_2))\cos\phi_q(y,t_1)\sin\phi_q(y,t_2)\rangle_0. \end{aligned} \tag{12}$$

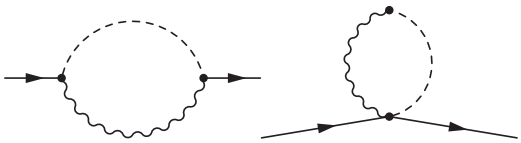

FIG. 2. Lowest-order diagrams for the retarded self energy $\Sigma_R(\omega)$. Dashed lines correspond to disorder average $\langle\xi(x)\xi^*(y)\rangle$ and wavy lines correspond to averaging of sines cosine and cosines of boson fields. Solid lines correspond to "amputated" external Green function lines

By $\langle\dots\rangle_0$ we denote the average with respect to the free boson action. This analytic expression corresponds to two Feynman diagrams (see Fig. 2).

Performing the average of sines and cosines of ϕ fields using Wicks theorem, we extract the retarded bosonic self-energy, whose Fourier transform reads

$$\Sigma_R(\omega) = -\frac{4D}{\pi^2 a^2}\int_0^\infty dt(1-e^{i\omega t})e^{2i(G_K(t)-G_K(0))}\sin 2G_R(t), \tag{13}$$

where the bare retarded and Keldysh components of the Green function are as follows:

$$G_R^{(0)}(\omega,q) = \frac{\pi u K}{(\omega+i0)^2-u^2q^2}, \tag{14}$$

$$G_R^{(0)}(t,x) = -\frac{\pi K}{2}\theta(t)\theta(ut-|x|), \tag{15}$$

$$G_K^{(0)}(\omega) = F(\omega)\left(G_R^{(0)}(\omega)-G_A^{(0)}(\omega)\right) \tag{16}$$

with $F(\omega)=\coth\frac{\beta\omega}{2}$ being the equilibrium distribution function. The inverse Fourier transformation of the Keldysh component $G_K^{(0)}(\omega)$ to the real space-time, $G_K^{(0)}(t,x)$, is infrared-divergent; it is sufficient to use the difference $G_K^{(0)}(t,x)-G_K^{(0)}(0,0)$, which is finite:

$$G_K^{(0)}(t,x)-G_K^{(0)}(0,0) = i\frac{K}{2}\ln\left(\frac{u^2\beta^2}{\pi^2\alpha^2}\left|\sinh\frac{\pi(x+ut)}{u\beta}\sinh\frac{\pi(x-ut)}{u\beta}\right|\right). \tag{17}$$

At low temperatures $T\ll J$, two different types of contributions to the disorder-induced self-energy can be separated: virtual transitions with $T\ll\omega\leqslant J$ and real (dissipative) transitions with $\omega\leqslant T$. The first contribution leads to a logarithmic renormalization of the model parameters yielding the RG equations (7) described above; the second contribution yields the dissipative behavior of the corresponding self-energy $\Sigma_R(\omega)=-i\omega/u\pi K\tau$ with a momentum relaxation rate as follows:

$$\frac{1}{\tau(T)} = \frac{2DK}{u}\frac{\Gamma^2(K)}{\Gamma(2K)}\left(\frac{2\pi aT}{u}\right)^{2K-2}. \tag{18}$$

According to Eq. (18), the product $T\tau\propto T^{3-2K}$ diverges as $T\to 0$ in the delocalized phase. The full Green function then reads as follows:

$$G_R(\omega,q) = \frac{\pi u K}{\omega^2-u^2q^2+i\omega/\tau}, \quad G_A=G_R^*. \tag{19}$$

A. Spin and heat conductivities

To obtain transport properties, one can apply the Kubo formulas. The expressions for spin and energy currents can be derived from the corresponding continuity equation $\partial_t\rho_\alpha+\nabla j_\alpha=0$ (index α corresponds to either spin or energy), and using classical equations of motion. For the Hamiltonian of the form $\hat H=\int dx\rho_E(\phi(x),\nabla\phi(x),\Pi(x))$, the equations of motion read as follows:

$$\partial_t\phi = \frac{\partial\rho_E}{\partial\Pi}, \quad \partial_t\Pi = -\frac{\partial\rho_E}{\partial\phi}+\nabla\frac{\partial\rho_E}{\partial(\nabla\phi)}, \tag{20}$$

so the energy density obeys the following continuity equation:

$$\partial_t\rho_E = \frac{\partial\rho_E}{\partial\phi}\partial_t\phi+\frac{\partial\rho_E}{\partial\nabla\phi}\partial_t\nabla\phi+\frac{\partial\rho_E}{\partial\Pi}\partial_t\Pi = \nabla\left(\frac{\partial\rho_E}{\partial\nabla\phi}\frac{\partial\rho_E}{\partial\Pi}\right) \tag{21}$$

and similarly for the spin density. Considering the total Hamiltonian consisting of two contributions (3) and (5), we arrive at the following expressions for the currents:

$$j_s = \frac{1}{\pi}\partial_t\phi, \quad j_E = -\frac{u}{\pi K}\partial_t\phi\nabla\phi. \tag{22}$$

We emphasize that Eq. (22) provide exact (within the Luttinger liquid approximation) expressions for both spin and thermal currents. Surprisingly, in the LL approximation, the energy current does not contain any terms related to the presence of backscattering. In Appendix, we provide a detailed derivation of the energy current, starting from the lattice fermion model (1), and show that backscattering does produce additional terms for the energy current, but these terms vanish in the continuous LL limit, when $a\to 0$ at some fixed value of the product Ja.

Spin transport is governed by the single-plasmon Green function, while for energy transport we need to calculate the correlation function of four ϕ fields. Applying the Kubo formula for spin conductivity, we reproduce the Drude-like result of Refs. [23,27],

$$\sigma(\omega) = \frac{i\omega}{\pi^2}G_R(\omega,q=0) = \frac{uK}{\pi}\frac{\tau}{1-i\omega\tau}, \tag{23}$$

valid at $\omega\ll T$.

The thermal conductivity κ is expressed in terms of the so-called "thermal susceptibility" $\chi_E(\omega,q)$ as $\kappa(\omega)=-i\beta/\omega\times(\chi_E(\omega,q=0)-\chi_E(0,0))$. Introducing the short notation $\mathbf{x}=(t,x)$, and $\mathbf{q}=(\omega,q)$, the expression for the thermal susceptibility in real space reads as follows:

$$\chi_E(\mathbf{x}_1-\mathbf{x}_2) = i\frac{u^2}{\pi^2K^2}\langle(\partial_t\phi\nabla\phi)_{cl}(\mathbf{x}_1)(\partial_t\phi\nabla\phi)_q(\mathbf{x}_2)\rangle, \tag{24}$$

and $\chi(\mathbf{q})$ is the Fourier transform of this expression. Applying Wicks theorem, one finds

$$\begin{aligned}\chi_E(\mathbf{x}_1-\mathbf{x}_2) \equiv -i\frac{u^2}{2\pi^2K^2}\big(&\partial_t^2G_K(\mathbf{x}_1-\mathbf{x}_2)\nabla^2G_A(\mathbf{x}_2-\mathbf{x}_1)\\ &+\partial_t\nabla G_R(\mathbf{x}_1-\mathbf{x}_2)\partial_t\nabla G_K(\mathbf{x}_2-\mathbf{x}_1)\\ &+\partial_t^2G_R(\mathbf{x}_1-\mathbf{x}_2)\nabla^2G_K(\mathbf{x}_2-\mathbf{x}_1)\\ &+\partial_t\nabla G_K(\mathbf{x}_1-\mathbf{x}_2)\partial_t\nabla G_A(\mathbf{x}_2-\mathbf{x}_1)\big).\end{aligned} \tag{25}$$

Here, we dropped the so-called contact term due to contraction $\langle\partial_t\phi_1\partial_t\phi_2\rangle\neq-\partial_t^2\langle\phi_1\phi_2\rangle$, since it does not contribute

to the conductivity. Performing a Fourier transformation of this expression and using the equilibrium relation for the Keldysh Green function (16), which holds also for the dressed propagators, and introducing a short notation $\mathbf{p} = (\epsilon, p)$, we arrive at

$$\chi_E(\mathbf{q}) = -i\frac{u^2}{4\pi^2 K^2}\int \frac{d^2\mathbf{p}}{(2\pi)^2}(\epsilon(p-q)+(\epsilon-\omega)p)^2 \times ((F(\epsilon)-F(\epsilon-\omega))G_R(\mathbf{p})G_A(\mathbf{p}-\mathbf{q}) + F(\epsilon-\omega)G_R(\mathbf{p}-\mathbf{q})G_R(\mathbf{p}) - F(\epsilon)G_A(\mathbf{p})G_A(\mathbf{p}-\mathbf{q})). \quad (26)$$

The second line of this expression contains products of two retarded (RR) or two advanced (AA) propagators. These terms do not contribute to the thermal conductivity; moreover, they are canceled by the term $\chi_E(\mathbf{q}=0)$ in the expression for the thermal conductivity. Then the result for the static thermal conductivity reads

$$\kappa = \frac{u^2}{\pi^2 K^2}\frac{1}{2T^2}\int\frac{d\epsilon}{2\pi}\frac{\epsilon^2}{\sinh^2\frac{\epsilon}{2T}}\int\frac{dp}{2\pi}p^2 G_R(\epsilon,p)G_A(\epsilon,p). \quad (27)$$

An integration in Eq. (27) with full propagators (19) yields the final result

$$\kappa = \frac{\pi}{3}uT\tau. \quad (28)$$

A comparison between Eqs. (23) and (28) provides us with the value of the Lorentz number

$$L = \frac{\kappa}{\sigma T} = \frac{\pi^2}{3K}. \quad (29)$$

We mention in passing, that formally the result (29) matches its standard Fermi liquid value $L_{\rm FL} = \frac{\pi^2}{3}$ for $K = 1$; however, in this range of K, our treatment of the spin chain problem is not applicable due to localization effects. Our result coincides with the one known for the clean limit of LL [26], but differs from the strong-impurity result by Kane and Fisher [26], $L_{\rm KF} = \pi^2/(2K + K^2)$. It is also different from the one obtained by Li and Orignac (LO) by means of memory function [27]: $L_{\rm LO} = \pi^2/9 \times (2K^{-1} + K^{-2})$. The coincidence of our result with the one obtained [26] for a single weak scatterer is expected, since (i) no multiple impurity effects were considered and (ii) we consider weak impurities and the renormalization flow at $K > 3/2$ makes it even weaker.

The discrepancy of our result with the LO result is due to limitations of the memory function formalism used in Ref. [27], which is based upon the extrapolation from the large-ω region to the static limit. Indeed, the frequency-dependent thermal conductance $\kappa(\omega)$ depends on two different frequency scales, T and $1/\tau$; according to Eq. (18), in the region $K > 3/2$, one always has $T \gg 1/\tau(T)$ in the low-temperature limit. In order to obtain the static thermal conductivity, one should be able to compute $\kappa(\omega)$ at $\omega\tau \ll 1$, whereas the memory function method is based upon the calculation of the high-frequency limit $\kappa(\omega \geqslant T)$ and further extrapolation to zero frequency. We believe that the presence of two parametrically different frequency scales $1/\tau$ and T makes such an extrapolation unreliable, which led LO to a result that is in error in the range of large $T\tau$ we are interested in.

The above calculation leading to Eqs. (28) and (29) should be performed, in general, with the parameters (g, K) renormalized [due to RG equations (7)] down to the temperature scale ξ_T. If the bare parameters (g, K) are in the bulk of the delocalized phase (not too close to the transition line), one can neglect the renormalization of K and u due to disorder, leading to results for spin and thermal conductivities that depend on the scale ξ_T via the scattering time τ only, see Eq. (18). Then the result is given by Eqs. (23) and (28) with bare parameters.

Near the transition line one should take the renormalization of all the parameters simultaneously. Below, we will see how it affects the physical properties of the system.

B. Vicinity of the point $\Delta = \frac{1}{2}$

Expanding the first integral of system (7) by $K - \frac{3}{2}$, or, equivalently, $\Delta - \frac{1}{2}$, one obtains

$$I - I_c = \frac{27}{\pi^2}\left(\Delta - \frac{1}{2}\right)^2 - \frac{16}{3\pi}\gamma. \quad (30)$$

The equality $I = I_c$ yields the phase boundary of the delocalized state in the form $(\Delta - \frac{1}{2})^2 = \frac{16\pi}{81}\gamma$.

The solution of equations (7) can be expressed in terms of the vicinity to the transition line $\alpha = \sqrt{I - I_c} \ll 1$:

$$u(\xi) = u\exp\left(\frac{2}{3}K(\xi) - 1\right)$$
$$K(\xi) = \alpha\coth\alpha(\xi + \xi_0)$$
$$g(\xi) = \frac{8\alpha^2}{9\sinh^2\alpha(\xi+\xi_0)}, \quad (31)$$

where ξ_0 depends on the initial values of parameters. Considering the temperature to be low enough (so $\xi_T \gg |\xi_0|, 1/\alpha$), one obtains the low-temperature behavior of the renormalized parameters $g(\xi_T) \simeq \alpha^2\exp(-2\alpha\xi) \simeq \alpha^2(T/J)^{2\alpha}$ and $K(\xi_T) - \frac{3}{2} \simeq \alpha = \text{const}$.

Now we repeat the above calculations leading to nonzero $\mathrm{Im}\Sigma(\omega)$ and obtain Drude-type formulas with corrected power-law exponent α:

$$\sigma \simeq \alpha^{-2}a(T/J)^{-1-2\alpha}, \quad \kappa \simeq J\alpha^{-2}a(T/J)^{-2\alpha}. \quad (32)$$

The Lorentz number is still given by Eq. (29) once renormalization $K \to K(\xi_T)$ is taken into account. Modifications of K and α are negligible if $g \ll (K - \frac{3}{2})^2$.

C. Smallness of the interference corrections

Our result for the heat conductance, Eq. (28), was obtained within a Drude-type approximation. Since our system is one-dimensional, some care should be exercised to check if the effects of quantum interference and Anderson localization could affect that result. To begin with, it is useful to employ the result of Ref. [22] where the same issue was considered for a disordered Luttinger liquid with a weak interaction, $|K - 1| \ll 1$. Namely, it was found in Ref. [22] that interference corrections are negligible at sufficiently high temperatures $T \geqslant \tau^{-1}(T)(K-1)^{-2}$. We are working at $K > 3/2$ and the corresponding condition is just $T \gg 1/\tau(T)$, which is always fulfilled at low temperatures $T \ll J$ according to Eq. (18).

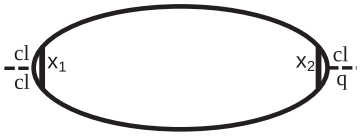

FIG. 3. Loop diagram for "thermal susceptibility" χ_E. Thermal current vertices act as the following combinations of derivatives: $(\partial_t\nabla' + \partial_t'\nabla)$, with derivatives ∂_t, ∇ acting on one ϕ field in the vertex and ∂_t', ∇' acting on another one. Solid lines correspond to "dressed" Green functions.

To estimate the interference corrections more accurately, we examine the expression for the "thermal susceptibility" to higher orders in $S_{\rm dis}$ adding impurity lines connecting the upper and lower Green functions drown in Fig. 3. The first-order correction (with single impurity line) vanishes at zero external momentum due to the gradient structure of the energy current vertex. The first nontrivial corrections are due to diagrams shown in Fig. 4; the corresponding analytical expressions yield

$$\begin{aligned}\delta\chi_E(t-t',x-x') &= \frac{1}{2}\left(\frac{iD}{\pi^2\alpha^2}\right)^2 \int dt_1dt_2dt_3dt_4dydz\langle\partial_t\phi_{cl}(x,t)\nabla\phi_{cl}(x,t)\\ &\times(\partial_t\phi_{cl}(x',t')\nabla\phi_q(x',t') + \partial_t\phi_q(x',t')\nabla\phi_{cl}(x',t'))\\ &\times\cos(2\phi_{cl}(y,t_1) - 2\phi_{cl}(y,t_2))\sin\phi_q(y,t_1)\sin\phi_q(y,t_2)\\ &\times\cos(2\phi_{cl}(z,t_3) - 2\phi_{cl}(z,t_4))\sin\phi_q(z,t_3)\sin\phi_q(z,t_4)\rangle_0. \end{aligned} \quad (33)$$

Grayed box corresponds to sine and cosine averages and consists of an infinite number of boson propagators connecting all the points. Generally speaking, such box depends on all the ingoing energies and momenta. However, a direct calculation shows that it contains factors $e^{2i(G_K(t_i-t_j)-G_K(0))} \propto 1/\sinh^{2K}\pi T(t_i-t_j)$, which impose an effective constraint for the time differences: any such diagram is very small unless the condition $|t_i - t_j| \leqslant 1/T$ is fulfilled. On the other hand, a typical time scale for the dressed "external" [with respect to (w.r.t.) to the "grey area"] propagators is $\tau(T) \gg 1/T$; therefore, up to the leading order in $1/T\tau(T) \ll 1$, one can try to shrink all four space-time impurity points in Fig. 4 into a single one (see Fig. 5). However, the calculation of the remaining integrals yields zero result, due to the vector structure of the current vertex. Therefore nonzero vertex corrections appear in the next order in $1/T\tau(T) \ll 1$ only, and are small at low T in the whole "delocalized" phase $K > 3/2$.

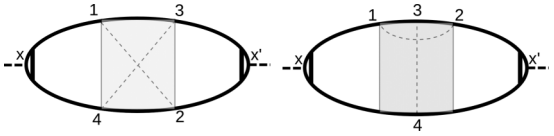

FIG. 4. Nontrivial corrections to "thermal susceptibility." Solid lines correspond to "dressed" Green functions, dashed lines correspond to the same impurity, and the grayed area corresponds to average of cosine and sine of ϕ fields. See main text for the analytical expressions.

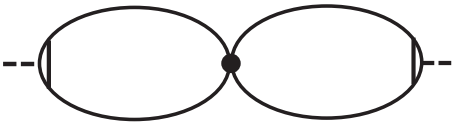

FIG. 5. Effective form of the diagram for the vertex correction to thermal susceptibility, valid in the leading order of expansion over $1/T\tau(T) \ll 1$.

D. Spectrum nonlinearity effects

At the Heisenberg isotropic point $\Delta = 1$ in the clean system, the spectrum of excitations is quadratic and the system is no longer described by a Luttinger liquid model. In the vicinity to this point, the plasmon velocity vanishes as $u = Ja\sqrt{(1-\Delta)/2}$; since the dimensionless disorder strength g depends on the velocity u and the interaction parameter K, see Eq. (6), this narrows the region where perturbation theory in powers of small g is applicable to $\langle h^2\rangle/J^2 \ll (1-\Delta)^{3/2}$.

However, spectrum nonlinearity effects at finite temperatures might become relevant long before the critical point $\Delta = 1$. Let us make some estimates. Due to particle-hole symmetry, only odd powers in quasiparticle spectrum survive; the first nonvanishing contribution to the dispersion relation will be $\delta\epsilon \sim \frac{u}{a}(ka)^3$. At finite temperatures, this yields a new energy scale $\delta\epsilon \sim T(Ta/u)^2$; such energy scale should be compared with the scattering ratio $1/\tau \sim ug/a(T/J)^{2K-2}$. Therefore we conclude that spectrum nonlinearity will be important and should be taken into account when $(T/J)^{5-2K} \geqslant \langle h^2\rangle/J^2$.

For $K < 5/2$, it leads to a threshold for the temperature above which nonlinearity effects are expected to be important, $T_* \sim J(\langle h^2\rangle/J^2)^{1/(5K-2)}$; on the contrary, at $K > 5/2$, nonlinearity is always important at low temperatures. In terms of the Δ parameter, the borderline at $K = 5/2$ corresponds to $\Delta = \cos\pi/5 = (1+\sqrt{5})/4 \approx 0.81$.

IV. CONCLUSIONS

We have analyzed the spin and thermal conductance of an XXZ spin chain with random-field disorder in the parameter region where the major source of disorder (backscattering of Jordan-Wigner fermions) is suppressed by quantum fluctuations and irrelevant in the RG sense at low temperatures. Within the standard bosonization scheme, the problem is reduced to the Luttinger liquid model with a linear spectrum $\varepsilon(k) \simeq uk$ and Luttinger interaction parameter K in the range $3/2 < K < \infty$, which corresponds to $1/2 < \Delta < 1$ in terms of the original anisotropy parameter $\Delta = J_z/J$ of the spin chain. We derive a phase boundary in terms of Δ and normalized disorder $\langle h^2\rangle/J^2$ and compare it with the numerical result of Ref. [18]. Then we used a diagrammatic Drude-like calculation of thermal and spin conductivities and found a Lorentz number, see Eq. (29), different from the previous result [27]. We also argue that quantum interference (the effects beyond Drude approximation) is irrelevant at low temperatures due to strong enough inelastic scattering at $1/2 < \Delta < 1$.

These results were obtained neglecting forward scattering of Jordan-Wigner fermions by disorder, which is allowed as long as the approximation of LL model with linear spectrum is employed. However, this approximation is not evidently

correct everywhere in the delocalized phase. We estimated a region where it might lead to a qualitatively different low-temperature behavior as $\Delta > \cos\frac{\pi}{5}$. The effects of spectrum nonlinearity will be considered in a separate publication.

We have not studied the region $\Delta < \frac{1}{2}$ where localization due to disorder is expected; here, it is very interesting to consider the close vicinity of the transition point, $\frac{1}{2} - \Delta \ll 1$ and $\langle h^2\rangle/J^2 \ll 1$ and search for the existence of a localization-delocalization threshold as a function of the excitation energy, like the one studied in Refs. [20,28] for the Bethe lattice model.

ACKNOWLEDGMENTS

This research was supported by the Russian Foundation for Basic Research via Grant No. 13-02-00963 (general analysis of the phase diagram, Fig. 1) and by the Russian Science Foundation via Grant No. 14-42-00044 [all other results, presented in Eqs. (28), (29), and (32)]. We are grateful to I. V. Kolokolov, V. E. Kravtsov, K. Michaeli, L. B. Ioffe, and K. S. Tikhonov for useful discussions.

APPENDIX: DERIVATION OF THE ENERGY CURRENT STARTING FROM THE LATTICE MODEL

We study a general Hamiltonian which is a sum of local on-site energy operators $H = \sum_n h_{n,n+1}$, with on-site energies that satisfy the continuity equation $\partial_t h_{n,n+1} + j_{E,n+1} - j_{E,n} = 0$ with an energy current $j_{E,n} = i[h_{n-1,n}, h_{n,n+1}]$. For the particular Hamiltonian (1), on-site energies have the form

$$h_{n,n+1} = -J\left[\hat{S}^x_n\hat{S}^x_{n+1} + \hat{S}^y_n S^y_{n+1} + \Delta\hat{S}^z_n\hat{S}^z_{n+1}\right] + h_n\hat{S}^z_n. \quad \text{(A1)}$$

Substituting this expression into the expression for the energy current yields two contributions. The first contribution is of kinetic nature, it does not contain disorder and can be written in a compact form as a determinant:

$$j^{(kin)}_{E,n} = \det\begin{pmatrix} \hat{S}^x_{n-1} & \hat{S}^x_n & \hat{S}^x_{n+1} \\ \hat{S}^y_{n-1} & \hat{S}^y_n & \hat{S}^y_{n+1} \\ \Delta\hat{S}^z_{n-1} & \hat{S}^z_n & \Delta\hat{S}^z_{n+1} \end{pmatrix}. \quad \text{(A2)}$$

Below, we will focus only on the second term, which contains disorder. The corresponding expression in the original spin representation and in the Jordan-Wigner representation reads as follows:

$$\begin{aligned} j^{(dis)}_{E,n} &= -i\frac{J}{2}h_n(S^+_{n-1}S^-_n - S^-_{n-1}S^+_n) \\ &= -i\frac{J}{2}h_n(c^\dagger_{n-1}c_n - c^\dagger_n c_{n-1}). \end{aligned} \quad \text{(A3)}$$

The next step is to take the continuum limit by replacing the lattice operators c_n with the continuous field $\psi(x = na) = c_n/\sqrt{a}$ and replacing fields h_n with the continuous potential $V(x = na) = h_n$. The corresponding expression for the energy current density then reads as follows:

$$j^{(dis)}_E(x) = -i\frac{Ja}{2}V(x)(\psi^\dagger(x-a)\psi(x) - \psi^\dagger(x)\psi(x-a)). \quad \text{(A4)}$$

In order to separate forward and backward scattering, we introduce slowly varying in space left- and right-moving fermionic fields $\psi_{L,R}(x)$ with $\psi(x) = e^{ik_F x}\psi_R(x) + e^{-ik_F x}\psi_L(x)$. After splitting the potential $V(x)$ onto a "forward-scattering" part $\eta(x)$ with Fourier harmonics $q \sim 0$ and a "backward-scattering" part $\xi(x)$ with $q \sim 2k_F$, one obtains the contributions to the energy current from forward- and backward-scattering processes:

$$\begin{aligned} j^{(f.s.)}_E &= \frac{Ja}{2}\eta(x)(\psi^\dagger_R(x-a)\psi_R(x) - \psi^\dagger_L(x-a)\psi_L(x)) + \text{H.c.} \\ &\approx Ja\eta(x)(\psi^\dagger_R(x)\psi_R(x) - \psi^\dagger_L(x)\psi_L(x)), \end{aligned} \quad \text{(A5)}$$

$$\begin{aligned} j^{(b.s.)}_E &= \frac{Ja}{2}\xi^*(\psi^\dagger_R(x-a)\psi_L(x) - \psi^\dagger_R(x)\psi_L(x-a)) + \text{H.c.} \\ &\approx \frac{Ja^2}{2}\xi^*(-\nabla\psi^\dagger_R\psi_L + \psi^\dagger_R(x)\nabla\psi_L) + \text{H.c.} \end{aligned} \quad \text{(A6)}$$

One can see that the backward-scattering contribution is of the next order in the small lattice constant a and indeed vanishes in the continuum limit, that is, $a \to 0$ keeping $u \propto Ja$ constant.

[1] D. M. Basko, I. L. Aleiner, and B. L. Altshuler, Ann. Phys. **321**, 1126 (2006).
[2] I. V. Gornyi, A. D. Mirlin, and D. G. Polyakov, Phys. Rev. Lett. **95**, 206603 (2005).
[3] R. Nandkishore and D. A. Huse, Ann. Rev. Condens. Matter Phys. **6**, 15 (2015).
[4] A. Pal and D. A. Huse, Phys. Rev. B **82**, 174411 (2010).
[5] M. Serbyn, Z. Papic, and D. A. Abanin, Phys. Rev. Lett. **111**, 127201 (2013).
[6] M. Serbyn, Z. Papic, and D. A. Abanin, Phys. Rev. Lett. **110**, 260601 (2013).
[7] R. Berkovits, Phys. Rev. B **89**, 205137 (2014).
[8] Y. Bar Lev, G. Cohen, and D. R. Reichman, Phys. Rev. Lett. **114**, 100601 (2015).
[9] A. V. Sologubenko, K. Gianno, H. R. Ott, A. Vietkine, and A. Revcolevschi, Phys. Rev. B **64**, 054412 (2001).
[10] N. Hlubek, P. Ribeiro, R. Saint-Martin, A. Revcolevschi, G. Roth, G. Behr, B. Buchner, and C. Hess, Phys. Rev. B **81**, 020405(R) (2010).
[11] N. Hlubek, P. Ribeiro, R. Saint-Martin, S. Nishimoto, A. Revcolevschi, S.-L. Drechsler, G. Behr, J. Trinckauf, J. E. Hamann-Borrero, J. Geck, B. Buchner, and C. Hess, Phys. Rev. B **84**, 214419 (2011).
[12] C. Karrasch, R. Ilan, and J. E. Moore, Phys. Rev. B **88**, 195129 (2013).
[13] Y. Huang, C. Karrasch, and J. E. Moore, Phys. Rev. B **88**, 115126 (2013).
[14] T. Giamarchi and H. J. Schulz, Phys. Rev. B **37**, 325 (1988).
[15] T. Giamarchi, *Quantum Physics in One Dimension* (Clarendon press, Oxford, 2003).
[16] Z. Ristivojevic, A. Petkovic, P. Le Doussal, and T. Giamarchi, Phys. Rev. Lett. **109**, 026402 (2012).
[17] G. Bouzerar and D. Poilblanc, J. Phys. I (France) **4**, 1699 (1994).

[18] P. Schmitteckert, T. Schulze, C. Schuster, P. Schwab, and U. Eckern, Phys. Rev. Lett. **80**, 560 (1998).
[19] J. M. Carter and A. MacKinnon, Phys. Rev. B **72**, 024208 (2005).
[20] M. V. Feigelman, L. B. Ioffe, and M. Mezard, Phys. Rev. B **82**, 184534 (2010).
[21] A. Klein and J. F. Perez, Commun. Math. Phys. **128**, 99 (1990).
[22] I. V. Gornyi, A. D. Mirlin, and D. G. Polyakov, Phys. Rev. B **75**, 085421 (2007).
[23] A. D. Mirlin, D. G. Polyakov, and V. M. Vinokur, Phys. Rev. Lett. **99**, 156405 (2007).
[24] B. Kramer and A. MacKinnon, Rep. Prog. Phys. **56**, 1469 (1993).
[25] A. Kamenev and A. Levchenko, Adv. Phys. **58**, 197 (2009).
[26] C. L. Kane and M. P. A. Fisher, Phys. Rev. Lett. **76**, 3192 (1996).
[27] M.-R. Li and E. Orignac, Europhys. Lett. **60**, 432 (2002).
[28] M. V. Feigel'man and L. B. Ioffe (unpublished).